129
9-19-75

a-1533

UCRL-51682, Pt. 7

BEHAVIOR OF POROUS BERYLLIUM UNDER THERMOMECHANICAL LOADING

Part 7: Calibration Studies on the Carbon Piezoresistive Gage

R. R. Horning
W. M. Isbell

June 17, 1975

Prepared for U.S. Energy Research & Development Administration under contract No. W-7405-Eng-48

MASTER

DISTRIBUTION OF THIS DOCUMENT UNLIMITED

NOTICE

"This report was prepared as an account of work sponsored by the United States Government. Neither the United States nor the United States Energy Research & Development Administration, nor any of their employees, nor any of their contractors, subcontractors, or their employees, makes any warranty, express or implied, or assumes any legal liability or responsibility for the accuracy, completeness or usefulness of any information, apparatus, product or process disclosed, or represents that its use would not infringe privately-owned rights."

Printed in the United States of America
Available from
National Technical Information Service
U. S. Department of Commerce
5285 Port Royal Road
Springfield, Virginia 22151
Price: Printed Copy $___*; Microfiche $2.25

*Pages	NTIS Selling Price
1-50	$4.00
51-150	$5.45
151-325	$7.60
326-500	$10.60
501-1000	$13.60

Distribution Category
UC-34

LAWRENCE LIVERMORE LABORATORY
University of California/Livermore, California/94550

UCRL-51682, Pt. 7

BEHAVIOR OF POROUS BERYLLIUM UNDER THERMOMECHANICAL LOADING

Part 7: Calibration Studies on the Carbon Piezoresistive Gage

R. R. Horning
W. M. Isbell

MS. date: June 17, 1975

NOTICE
This report was prepared as an account of work sponsored by the United States Government. Neither the United States nor the United States Energy Research and Development Administration, nor any of their employees, nor any of their contractors, subcontractors, or their employees, makes any warranty, express or implied, or assumes any legal liability or responsibility for the accuracy, completeness or usefulness of any information, apparatus, product or process disclosed, or represents that its use would not infringe privately owned rights.

Preface

This report is Part 7 of a seven-part series on Behavior of Porous Beryllium Under Thermomechanical Loading (UCRL-51682 Pts. 1-7). The titles and authors of the individual reports in the series are as follows:

	Title	Author
Part 1.	Summary of Results	W. M. Isbell
Part 2.	Quasi-Static Deformation	R. N. Schock, A. E. Abey, and A. G. Duba
Part 3.	Shock Wave Studies	W. M. Isbell and R. R. Horning
Part 4.	Constitutive Model for Wave propagation	F. H. Ree, W. M. Isbell, and R. R. Horning
Part 5.	Electron-Beam Studies	O. R. Walton and W. M. Isbell
Part 6.	Effect of Pressure on the Microstructure of Plasma-Sprayed Beryllium	J. E. Hanafee and E. O. Snell
Part 7.	Calibration Studies on the Carbon Piezoresistive Gage	R. R. Horning and W. M. Isbell

This work was supported by the Defense Nuclear Agency (Mr. Donald Kohler, technical monitor) under the auspices of the U.S. Energy Research & Development Administration.

BEHAVIOR OF POROUS BERYLLIUM UNDER THERMOMECHANICAL LOADING

Part 7: Calibration Studies on the Carbon Piezoresistive Gage

Abstract

The calibrations, time responses, and Hugoniot for carbon piezoresistive gages from two manufacturers are presented. These gages exhibit a high sensitivity of about -20% resistance change per GPa at 0.5 GPa. Their equilibrium times, when tested in fused silica, exceed 0.6 μs below 0.5 GPa but improve at higher stresses and under better impedance matching conditions. They can be made of low atomic number materials, making them interesting candidates for studying the mechanical responses of materials to electron and x-ray deposition.

Introduction

One of several devices available to measure the response of materials to shock loading is the piezoresistive gage. The material most commonly used in these gages is Manganin,*[1-4] but sodium,[5] ytterbium,[6-8] calcium,[9] lithium,[9] carbon,[10,11] and others have also been tested.

All these piezoresistive materials have the common characteristic that they can be made into thin assemblies of relatively small area, permitting their use as "in-material"[12] gages. In this configuration, the sensitive element is placed between layers of the host material to be tested. Since the gage is quite thin (≈0.1 mm), it usually comes into pressure equilibrium with the material under test within a few hundred nanoseconds by a series of wave reverberations across the gage, even though the shock impedances of the gage and test specimen may be very different. Thus if a suitable calibration has been performed on the gage, one obtains a direct measure of the pressure in the test specimen. However, the impedance difference between the gage and host material does affect the profile shape, and accurate work requires the ability to calculate profiles using the equations of state of the gage and material under test.

Using "in-material" gages placed between successive layers of the specimen, one can study the evolution of waves as they propagate through the material. Elastic and plastic compressive and release wave profiles can be measured, and by using careful timing techniques, wave speeds can be obtained.

*Reference to a company or product name does not imply approval or recommendation of the product by the University of California or the U.S. Energy Research & Development Administration to the exclusion of others that may be suitable.

Carbon Gage Construction

The two gage types discussed here were made by different manufacturers. Both types are available in a variety of element sizes, lead materials and dimensions, and insulator materials and thicknesses. Differences in performance noted below are apparently due to the different compositions of the sensitive carbon elements, since other components of the gages are substantially the same. Only gages with a nominal 50-Ω static resistance are reported here.

The type-A gage, shown in Fig. 1, is made from a composition with comparatively low resistivity, as can be inferred from the aspect ratio of the sensitive element. The gage consists of the sensitive element, with its copper electrical leads, enclosed by a 0.025-mm-thick layer of type H Kapton* on each side. Epoxy resin is used to hold the assembly together. The total package thickness is approximately 0.09 mm.

Two sizes of the type-B gage were used, as shown in Fig. 1. Both were made from the same lots of raw materials to avoid batch-to-batch variation. The resistivity of the sensitive elements of these gages is higher than that of type A and thus the aspect ratio is different; however, the leads and Kapton insulation are similar for the two types. The package thickness measured at the active element is nominally 0.11 mm.

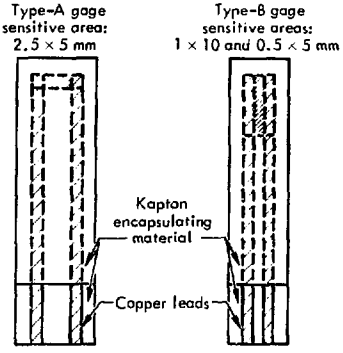

Fig. 1. Carbon piezoresistive gages. Both types are insulated on both sides by 25-μm-thick type-H Kapton film. Both have copper leads.

Experimental Technique

All data taken in the present work were generated on an 89-mm-diam gas gun using techniques similar to those described by other investigators including Thunborg et al.[13] Projectile velocities were measured with four charged electrical pins protruding from the side of the muzzle,[14] giving three measurements, which agreed within 1 % or better. Projectile tilt was measured on each shot using an array of four piezoelectric pins arranged around the periphery of the target (Fig. 2). These pins were struck by the impactor, mounted on the face of the projectile, and produced voltage pulses, which were recorded on raster oscilloscopes. The relative timing of these pulses permitted calculation of the impactor tilt. Timing accuracy between pins is estimated at ~5 ns. All shots except one had tilts of 1 mrad or less, resulting in tilt-induced rise times in the gages of 10 to 60 ns.

Gages were bonded* between flat plates of materials with known equations of state, taking

*DuPont trademark.

*The adhesive used was Hysol R8-238 (Dexter Corporation) epoxy resin with H2-3490 hardener. Adhesive thickness was approximately 5 μm on each side of the gage assemblies.

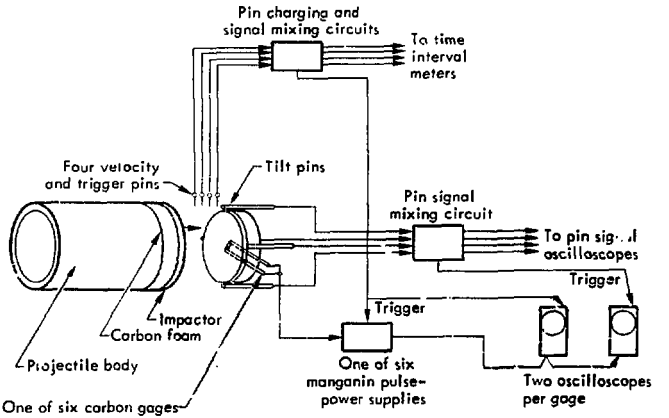

Fig. 2. Schematic representation of experimental setup.

care that no air bubbles were formed and that the plates remained parallel to one another within 0.3 mrad. These target assemblies were mounted in the gas gun and struck by projectiles on which were mounted impactor plates with known equations of state.

This work included experiments with gages bonded between plates of fused silica (Dynasil 5000), which were struck by fused silica, and experiments in porous, plasma-sprayed beryllium of two densities: 1.59 g/cm^3 and 1.66 g/cm^3. All impactors were supported by 0.2 g/cm^3 carbon foam in the projectile assembly.

For the fused silica experiments, six gages (three of each type) were sandwiched between a thin target plate (~1.5 mm) and a thicker plate (~12.7 mm) which transmitted the wave away from the gages. This configuration allowed all six gages to be stressed under essentially identical impact conditions.

Some experiments in porous beryllium also included six gages. For these tests, however, the gages were imbedded at four different levels within the porous material, including the impact surface. The beryllium plates were slotted to receive the gages, and gage spacing was such that the disturbance arising from the discontinuity represented by a gage did not reach an adjacent gage during the time of interest. The beryllium plates were struck by polymethyl methacrylate (PMMA) impactors.

A simplified schematic of the gage signal-recording system is also shown in Fig. 2. The gages were powered by Sandia Corporation, Model 600-50-75, Manganin pulse-power supplies, which include modified Wheatstone bridges to eliminate large dc offset voltages. Each gage signal was recorded using two oscilloscopes with one timed to permit continuous observation from power pulse turn-on through release wave passage. The bandwidth of the recording system was approximately 80 MHz.

Results

SOLID MATERIALS

Gage calibration data were obtained from experiments in which the gages were bonded between plates of fused silica. This calibration was accomplished using the Hugoniot of fused silica and the measured impactor velocities to calculate[15,16] peak stresses generated in the plates surrounding the gages. Fused silica was chosen as a host material for several reasons, including:

- The nonlinear elastic nature of the material (to ~2.8 GPa) gives rise to essentially flat-topped shock waves with rise and fall times of <10 ns under the test conditions employed.
- The Hugoniot of the material has been accurately measured and can be adequately simulated in hydrodynamic computer codes.
- The material is very reproducible.
- The transparent nature of fused silica allows visual inspection of the gage after assembly, thus avoiding errors from bubbles, bond separation, etc.

Hugoniot data reported by Barker and Hollenbach[17] were used.

Our experimental results are listed in Table 1. Figure 3 shows the corresponding calibration curves for the two gage types. In addition to our results, manufacturers' data and data taken by Shay and Copeland[18] of this Laboratory, are shown.

Least-squares curve fitting resulted in the following response functions for type-A gages over the indicated stress ranges:

Our fit to the manufacturers' data:

$$P = -1.306(\Delta R/R_0) + 11.77(\Delta R/R_0)^2 + 30.12(\Delta R/R_0)^3 + 40.54(\Delta R/R_0)^4 \pm 0.14 \text{ GPa} \quad (0 < P \leq 5.10 \text{ GPa}) \quad (1)$$

Shay and Copeland's data taken in 4340 steel

$$P = -2.495(\Delta R/R_0) - 2.329(\Delta R/R_0)^2 - 12.87(\Delta R/R_0)^3 \pm 0.062 \text{ GPa} \quad (0 < P \leq 1.69 \text{ GPa}) \quad (2)$$

Our data taken in fused silica:

$$P = 0.1\{-1 + \exp[-14.30(\Delta R/R_0) - 34.93(\Delta R/R_0)^2 - 53.14(\Delta R/R_0)^3 - 29.38(\Delta R/R_0)^4]\} \pm 0.106 \text{ GPa} \quad (0 < P \leq 3.43 \text{ GPa}). \quad (3)$$

Table 1. Carbon-gage calibration data taken in fused silica.

Shot No.	Projectile velocity (mm/μs)	Calculated stress (GPa)	Gage type	$\Delta R/R_0$
QE	0.5835	3.433	A	-0.5613
			A	-0.5794
			A	-0.5823
			B	-0.4691
			B	-0.4576
			B	-0.4733
QA	0.4654	2.779	A	-0.5220
			A	-0.5247
			B	-0.4261
			B	-0.4290
QB	0.3156	1.931	A	-0.4446
			A	-0.4630
			A	-0.4636
			B	-0.3833
			B	-0.3848
QC	0.1657	1.046	A	-0.3211
			A	-0.3049
			A	-0.3316
			B	-0.2937
			B	-0.2883
QD	0.0620	0.401	A	-0.1610
			A	-0.1661
			A	-0.1637
			B	-0.1535
			B	-0.1534
			B	-0.1535

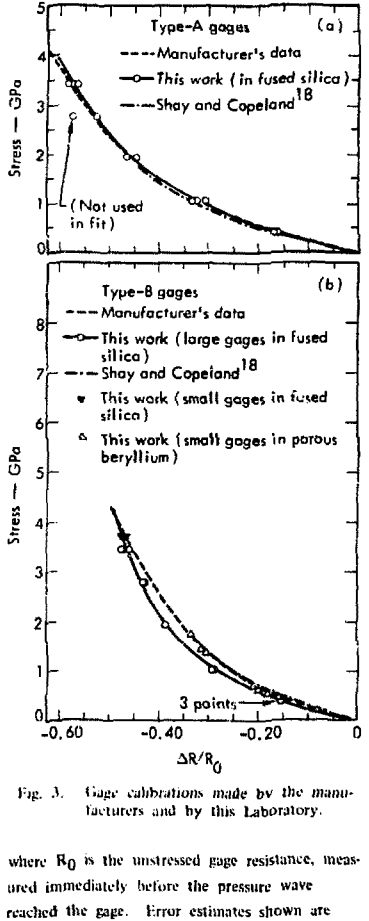

Fig. 3. Gage calibrations made by the manufacturers and by this Laboratory.

where R_0 is the unstressed gage resistance, measured immediately before the pressure wave reached the gage. Error estimates shown are quadratic mean errors in the fits.* Note that one data point showed sufficient deviation from the main body of data that it was not used in obtaining the least squares fit in fused silica. The reasons behind this anomalous data point were not evident.

Calibration functions for large type-B gages are:

Calibration function supplied by the manufacturer:

$$P = -2.68(\Delta R/R_0) - 2.10(\Delta R/R_0)^2 - 28.7(\Delta R/R_0)^3 \text{ GPa} \quad (0 < P \leq 18.7 \text{ GPa}) \quad (4)$$

Shay and Copeland's data taken in 4340 steel:

$$P = -2.837(\Delta R/R_0) - 1.248(\Delta R/R_0)^2 - 24.68(\Delta R/R_0)^3 \pm 0.019 \text{ GPa} \quad (0 < P \leq 1.54 \text{ GPa}) \quad (5)$$

Our data taken in fused silica:

$$P = 0.1\{-1 + \exp[-13.75(\Delta R/R_0) - 26.13(\Delta R/R_0)^2 - 28.13(\Delta R/R_0)^3]\} \pm 0.142 \text{ GPa} \quad (0 < P \leq 3.43 \text{ GPa}) \quad (6)$$

The three data points at 0.4 GPa (Fig. 3b) were obtained in a single experiment from gages that had not reached equilibrium before release waves from the rear of the impactors arrived at 1.0 μs after the compressive wave arrival (Fig. 4). Estimates of the equilibrium values of $\Delta R/R_0$, i.e., values that these gages might have reached for sufficiently long pulses, were used as input data for deriving Eq. (6). The uncertainty in these estimates is about 10%. Three type-A gages were also employed in this experiment. Two of these reached equilibrium about 0.6 μs after wave arrival. The third had not reached equilibrium at 1.0 μs. Impactor tilt in this experiment degraded the compressive wave rise time by less than 0.06 μs for each gage.

*The stated quadratic mean errors in our data are functions of data scatter and the degree to which the chosen functional forms can be adjusted to fit the data sets. The individual data points are estimated to have uncertainties of ±2% in fractional resistance change and in stress.

Stress wave profiles calculated from two of the waveforms of Fig. 4 are plotted in Fig. 5 along with a hydrodynamically calculated profile of stress in the gages. Both the gages and the theoretical wave profile show reverberations or "ring-up" to the leading edge of the waveform as the gages equilibrate with the surrounding material. Reverberations appear at 0.25 GPa and above in the calculated profile. The ability to resolve these small perturbations on the leading edge of the wave enabled us to construct a Hugoniot for the gage package, as discussed below.

The effect of nonzero strength in the carbon foam supporting the rear surface of the impactor is evident in that the calculated and the measured profiles do not return to zero stress after the passage of the wave. The fidelity of the gages in reproducing the release portion of the wave indicates that the gages do not exhibit excessive hysteresis upon release. The second peak in the profile, appearing at about 2.1 μs, is a reflected wave which made a round trip from the gage surface, through the first fused silica plate and impactor, and back to the gages again. Both types

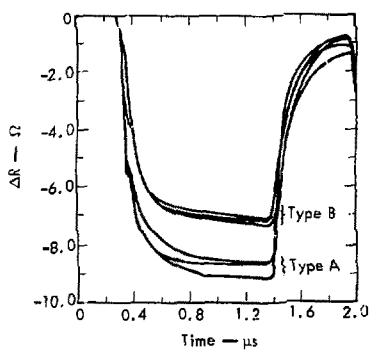

Fig. 4. Temporal responses of three type-A and three large type-B gages to the 0.40-GPa pulse shown in Fig. 5. The host material was fused silica.

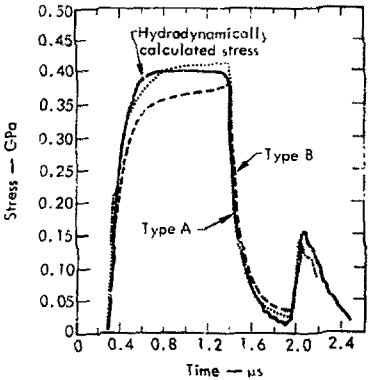

Fig. 5. Theoretical and experimental wave profiles calculated from one of the type-A and one of the type-B gage responses shown in Fig. 4.

of gages reproduced this detail reasonably well, indicating the ability of the gages to respond to subsequent stresses after an initial compressive release cycle.

In Fig. 6, we show calculations and data taken at 1.06 GPa. The type-A gage reached equilibrium within about 0.5 μs; another gage (not shown) responded in about 0.3 μs. Two type-B gages furnished data in this experiment. Both were near ($\geq$97%) equilibrium within 1.1 μs after shock arrival. At still higher stresses, the response times continued to decrease for both types of gages, as might be expected because of the higher wave speeds, and thus shorter equilibration times, achieved at higher stresses.

An effective Hugoniot for both types of gages was calculated from the structure evident on the compressive portions of the wave profiles (see Fig. 4). The stress in the gage equilibrated with the stress in the surrounding fused silica by a series of reverberations across the gage. Where the steps of increasing stress were sufficiently well

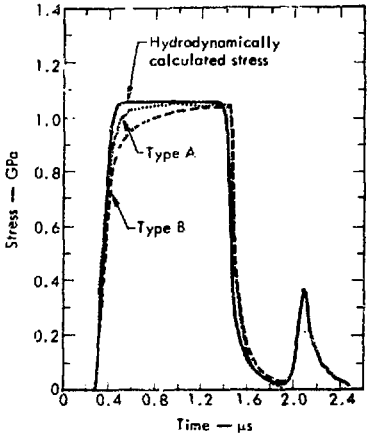

Fig. 6. Theoretical and experimental wave profiles calculated from one type-A and one type-B gage at a peak stress of 1.06 GPa.

defined, the Hugoniot jump conditions were used to determine the "average" Hugoniot of the gage package. Data were obtained in the range of 0.114 to 0.966 GPa. A least squares fit to the data is:

$$P = 2.24\ U_p + 4.70\ U_p^2 \pm 0.019\ \text{GPa}. \qquad (7)$$

where U_p is the particle velocity in km/s. This Hugoniot, along with an initial density, ρ_0, of 1.33 gm/cm^3, was used to represent the gages in our hydrodynamic calculations[19] of wave profiles. The fused silica Hugoniot used was that given in Ref. 17.

POROUS BERYLLIUM

Type-A and small type-B gages were also tested in porous beryllium as part of a program to characterize the response of the latter material to a variety of loading conditions.[20,21] One point of interest was the possibility that, because of microstretching of the carbon element by the action of the pores, the gages might exhibit a different calibration in porous material than in solid material. A series of tests were performed in which an X-cut quartz gage was launched against a porous beryllium target containing a carbon gage. The conclusion of this study was that, for the carbon gages and material tested, no anomalous effect was found. Our type-A gage calibrations in fused silica and porous beryllium agreed within experimental error. The small type-B gage calibration agreed with the calibrations obtained by the manufacturer and by Shay and Copeland in solids (Fig. 3b).

Figure 7 illustrates the use of four small type-B gages to observe the evolution of a wave propagating through porous beryllium after impact by PMMA. The "X" values indicate the distance of propagation through the beryllium specimen. Note that one gage was located at the impact surface. The peak stresses measured by the gages agreed within experimental error with those calculated hydrodynamically throughout the stress range measured in porous beryllium (0.5 to 1.7 GPa). The gages performed satisfactorily, with no evidence of premature gage failure or of anomalous resistance changes caused by microstretching of the carbon element by the porous structure of the beryllium.

Application Considerations

Carbon gages have a large magnitude, negative thermal coefficient of resistance compared to Manganin gages. If electrical power levels of hundreds of watts are applied, as is common with Manganin and other comparatively low-sensitivity gages, carbon gages will decrease in resistance by a few percent in 10 or 20 μs. Thus, for precise work, the user should apply as little electrical energy to the gages before impact as possible and/or measure the gage resistance from power pulse turn-on to pressure wave arrival. For the calibration functions derived in this work, the resistances were measured immediately before pressure wave arrival.

As a matter of practical interest, type-A gages showed more variations in calibration within a manufacturing lot than did type-B gages. This variation is illustrated in Fig. 4 for a comparatively low stress. This difference was observed throughout the range of stresses used. On the other hand, the type-A gages showed somewhat faster time response, as discussed below.

As with other in-material gages, carbon gages exhibit a capacitive effect associated with compression of the insulating dielectric by metallic host materials. In the case of Manganin gages, this effect results in a negative spike at the beginning of an otherwise positive signal. The effect is more insidious in carbon gages, because

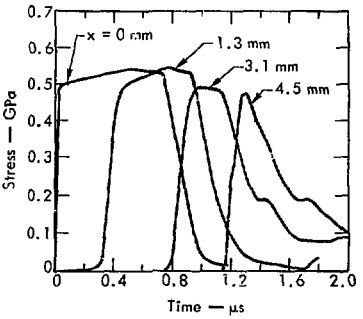

Fig. 7. Evolution of a pressure wave propagating through porous beryllium struck by 1.27-mm-thick polymethyl methacrylate, as observed using four carbon gages at different depths in a single experiment. X is the distance from the impact surface to the plane of the gage.

the increase in capacitance in parallel with the sensitive element results in the same reduction in impedance that is characteristic of the negative piezoresistive effect in the gage. Thus, careful interpretation of experimental records is usually required to distinguish between low-level precursor waves and the capacitive effect in metallic specimens. Interpretation of the slowly rising baseline occurring in the records for the three gages in Fig. 7 is representative of this problem.

Discussion

The type-A gage calibrations obtained by the manufacturer, Shay and Copeland, and us have shown excellent consistency (Fig. 3a). These calibrations have all been accomplished with gas guns, but using a variety of materials. The manufacturer used PMMA, 7075-T6 aluminum, 6%Al-4%V-90%Ti alloy, 2024-T3 aluminum, brass, and fused silica. Shay and Copeland used 4340 steel; and we used fused silica and porous beryllium. The slight divergence between the manufacturer's calibration and our own above 2 GPa is within the gage-to-gage repeatability.

Experiments were conducted on the large type-B gages by three groups, Naumann,[16] Shay and

Copeland,[18] and us. The latter two used similar gas gun techniques, while Naumann used an exploding foil facility[22] to generate short-duration, high-amplitude stress waves.

As shown in Fig. 3b, the results of Naumann's study and the Shay and Copeland study were quite similar, while our results, consistent within themselves, are quantitatively different. It is likely that this difference arises from batch-to-batch variations of the gages rather than differences in experimental techniques.

The small type-B gages we tested in porous beryllium exhibited a calibration very similar to those obtained for large gages by the other investigators. We tested only three small gages in fused silica (at 3.71 GPa), again with results which agreed well with the manufacturer's.

Additional data taken with large and small type-B gages in materials with known equations of state might be very useful in evaluating batch-to-batch repeatability and gage sensitivity to host material and gage size. In any case, we suggest that other investigators may wish to verify the calibration of their type-B gages.

The functional form that we have used in fitting our calibration data, a product of exponentials, Eqs. (3) and (6), is more complex than the polynomials chosen for the other calibrations and gives similar results over the range of our data. We have chosen this form because it tends to produce a curve with fewer observable inflection points near the origin than do the polynomials we have attempted to use. Thus, the product of exponentials has resulted in slightly better fits to our data at low stresses.

The temporal response of carbon gages insulated by Kapton is a complex function of stress, host material, and gage type. Data taken in fused silica indicate that the lower the stress, the slower the gages come to equilibrium. The equilibration time of type-A gages is approximately 0.2 μs above 1 GPa, although individual records showed response times greater than this value. The response time of type-B gages is somewhat longer, possibly because of their slightly greater thickness. An average response time of 0.2 μs is not achieved until a stress of about 2 GPa in fused silica.

Under impedance-matched conditions in which the shock impedance of the gage is equal to that of the host material, the gage should remain essentially in pressure equilibrium with the surrounding host. This equilibrium would hold exactly if the gage were made of a single, homogeneous material having no strain rate effects. In this idealized case, gage response time should be defined entirely by parasitic reactances and would be very fast compared to the gages studied here.

Thus we should expect faster carbon gage response when the shock impedances of the gage assembly and of the host material are more nearly equal than when the gages are tested in fused silica. Indeed, this faster response was exhibited when both types were used in porous beryllium, as was noted above for small type-B gages.

However, even with near-perfect impedance matching, neither type gage has a reactance-limited response for low stress levels. Both Naumann[10] and Charest[11] have published waveforms produced by carbon gages with Kapton insulation and with PMMA used as the host material. (PMMA has a Hugoniot and an initial density which are very similar to those of carbon-Kapton gages.) In both reports, the gages exhibited initially fast responses (about 0.2 μs to reach 95% of full amplitude at stresses below 0.5 GPa). However, nearly all low-stress waveforms that should have been flat-topped exhibited ramped tops. In fact, Naumann's shot 2841 had two carbon-Kapton gages with ramped tops lasting 10 μs at 0.21 GPa.

Within our experimental error, the same Hugoniot applies to both types of gages, even though they have different pressure-sensitive elements. This

result is not unreasonable because the gage-assembly specific volumes differ by only about 1.6% (0.754 cm^3/g for type A and 0.766 cm^3/g for type B), which is well within the uncertainty in the data points. The range of the Hugoniot data was limited to slightly less than 1 GPa. This limitation existed because reverberation wave speeds were so high at higher stress levels that the steps in the leading edges of the wave profiles were too short to be resolved by the gages with their response time limitations.

We wish to note that the measurements described above were taken over a limited stress range (0 to 34.3 GPa). Because of the nature of the mathematical fits to the data, extrapolations to high stresses should be made with caution.

In summary, carbon gages have high sensitivity, making them particularly useful for low-stress work in noisy environments. However, their relatively slow response time at low stress can be troublesome for short pulses, particularly if there is a large impedance mismatch between the gages and the host material under test.

Acknowledgments

We wish to thank W. M. Shay and A. B. Copeland for their helpful comments and for sharing their data with us. J. A. Charest, J. W. Lyle, and W. J. Naumann shared many valuable discussions and recommendations. J. J. Dub, G. L. Hickman, and R. E. Neatherland did excellent jobs of experiment assembly and execution.

References

1. J. A. Fuller and J. H. Price, Nature 193, 262 (1962).
2. D. Bernstein and D. D. Keough, J. Appl. Phys. 35, 1471 (1964).
3. E. Barsis, E. Williams, and C. Skoog, J. Appl. Phys. 41, 5155 (1970).
4. L. M. Lee, J. Appl. Phys. 44, 4017 (1973).
5. R. L. Huddleston and R. E. Sladky, Sodium and Strontium Shock Pressure Transducer Technical Report, Union Carbide Corporation, Nuclear Division, Oak Ridge, Tenn., Y-12 Plant, Rept. Y-1673 (1969).
6. R. A. Stager and H. G. Drickamer, Science 139, 1284 (1963).
7. H. D. Stromberg and D. R. Stephens, J. Phys. Chem. Solids 25, 1015 (1964).
8. M. J. Ginsberg, Calibration and Characterization of Ytterbium Stress Transducers, Stanford Research Institute, Menlo Park, Calif., Rept. DNA2742F (1971), AD732778.
9. R. F. Williams and D. D. Keough, Bull. Am. Phys. Soc., Series II 12, 1127 (1967).
10. W. J. Naumann, Carbon Stress Gauge Development, Final Report, Effects Technology, Inc., Santa Barbara, Calif., Rept. DNA3027F (1973), AD909553L.
11. J. A. Charest, Development of the Carbon Shock Pressure Gauge, EG&G, Inc., Santa Barbara, Calif., Rept. DNA3101F (1973), AD913951L.
12. P. J. A. Fuller and J. H. Price, Brit. J. Appl. Phys. 15, 751 (1964).
13. S. Thunborg, G. E. Ingram, and R. A. Graham, Rev. Sci. Instr. 35, 11 (1964).
14. G. R. Fowles, G. E. Duvall, J. Asay, P. Bellamy, F. Feistman, D. Grady, T. Michaels, and R. Mitchell, Rev. Sci. Instr. 41, 984 (1970).
15. G. E. Duvall, "Shock Waves in Condensed Media," in Proc. of the International School of Physics, Enrico Fermi; Physics of High Energy Density (Academic Press, New York, 1971).
16. J. W. Taylor, "Experimental Methods in Shock Wave Physics," in Metallurgical Effects at High Strain Rates (Plenum Co., New York, 1973).
17. L. M. Barker and R. E. Hollenbach, J. Appl. Phys. 41, 4208 (1970).
18. W. M. Shay and A. B. Copeland, Lawrence Livermore Laboratory, private communication (1973).
19. M. L. Wilkins, Calculation of Elastic-Plastic Flow, Lawrence Livermore Laboratory, Rept. UCRL-7322, Rev. 1 (1969).
20. W. M. Isbell and R. R. Horning, Behavior of Porous Beryllium Under Thermomechanical Loading: Part 3. Shock Wave Studies, Lawrence Livermore Laboratory, Rept. UCRL-51682, Pt. 3 (1974).
21. F. H. Ree, W. M. Isbell, and R. R. Horning, Behavior of Porous Beryllium Under Thermomechanical Loading: Part 4. Constitutive Model for Wave Propagation, Lawrence Livermore Laboratory, Rept. UCRL-51682, Pt. 4 (1974).
22. R. E. Graham, R. E. Wengler, and D. V. Keller, Trans ISA 9, 133 (1970).

MBB/rt/lh/edas